Transfer of Twelve Charges Is Needed to Open Skeletal Muscle Na^+ Channels

BIRGIT HIRSCHBERG, ARTHUR ROVNER, MITCHELL LIEBERMAN, and JOSEPH PATLAK

From the Department of Molecular Physiology and Biophysics, University of Vermont, Colchester, Vermont 05446

ABSTRACT Voltage-dependent Na^+ channels are thought to sense membrane potential with fixed charges located within the membrane's electrical field. Measurement of open probability (P_o) as a function of membrane potential gives a quantitative indication of the number of such charges that move through the field in opening the channel. We have used single-channel recording to measure skeletal muscle Na^+ channel open probability at its most negative extreme, where channels may open as seldom as once per minute. To prevent fast inactivation from masking the voltage dependence of P_o, we have generated a clone of the rat skeletal muscle Na^+ channel that is lacking in fast inactivation (IFM1303QQQ). Using this mutant channel expressed in *Xenopus* oocytes, and the extra resolution afforded by single-channel analysis, we have extended the resolution of the hyperpolarized tail of the P_o curve by four orders of magnitude. We show that previous measurements, which indicated a minimum of six effective gating charges, may have been made in a range of P_o values that had not yet arrived at its limiting slope. In our preparation, a minimum of 12 charges must function in the activation gating of the channel. Our results will require reevaluation of kinetic models based on six charges, and they have major implications for the interpretation of S4 mutagenesis studies and structure/function models of the Na^+ channel.

INTRODUCTION

Voltage-dependent Na^+ channels alter their rates of transition between open and closed states when membrane potential changes. Hodgkin and Huxley (1952*b*) originally hypothesized that this voltage sensitivity could be due to charged structures within the membrane that could move through the membrane's electric field. Such movement would drive conformational change in the channel, give rise to gating currents (subsequently measured directly for voltage-dependent channels [Armstrong and Bezanilla, 1973]), and alter the open probability. This fundamental concept of Hodgkin and Huxley (1952*b*) still forms the basis for our current understanding of how such channels respond to membrane potential.

Address correspondence to Joseph Patlak at Department of Molecular Physiology and Biophysics, University of Vermont, 55a South Park Drive, Colchester, VT 05446.

J. GEN. PHYSIOL. © The Rockefeller University Press · 0022-1295/95/12/1053/16 $2.00
Volume 106 December 1995 1053–1068

Hodgkin and Huxley (1952*a*) also recognized that measuring the exponential increase in open probability as a function of membrane potential gives a quantitative indication of the channel's voltage sensitivity. The steepest section of this exponential rise is at hyperpolarized potentials where open probability is low. This "limiting slope" gives a lower bound for the effective number of charges that cross the membrane fully in changing the channel from its closed to open states (e.g., Almers, 1978). Hodgkin and Huxley initially measured this limiting slope and estimated that transfer of at least six charges were necessary to open the Na^+ channel. Others have refined this measurement, most notably by studying Na^+ channels treated with NBA or pronase to remove inactivation (Oxford, 1981; Stimers, Bezanilla and Taylor, 1985), but best estimates have consistently been in the range of four to seven total charges. The use of about six charges has therefore become conventional in models of Na^+ channel activation.

The cloning of Na^+ channels (Noda et al., 1984) has precisely defined their primary structure, and has rekindled interest in the number and effective charge of the channel's voltage sensors. The channel consists of four repeated domains, each with six membrane-spanning segments. The fourth of these in each domain (S4) has 5–7 charged amino acids within the membrane, and is thus well suited as a voltage sensing structure. Mutation of these charges to neutral residues reduces the voltage dependence of the channel, clearly demonstrating their central role in gating (Stühmer et al., 1989). However, many questions remain: What fraction of all these charges actually move through the membrane upon gating? What is the gating current for a single gate? Are all four domains involved in gating the channel? These questions are of current interest in order to understand how best to model Na^+ channel activation kinetics.

The "quantal" gating charge (i.e., from the movement of a single gate) in Na^+ channels has been estimated at 2.4 using nonstationary fluctuation analysis (Conti and Stühmer, 1989). If the total number of charges were six, then these measurements would imply that as few as two such gates were functional during activation. In K^+ channels, however, recent measurements have revised upward the gating charge estimates from the original estimates of about 5. Zagotta et al. (1994) used limiting slope measurements to show that a minimum of 12–16 charges must be transferred in order for the *Shaker* K^+ channel to open. The ratio of total gating current to channel number measured with fluctuation analysis (Schoppa et al., 1992) or toxin binding (Aggarwal and MacKinnon, 1995) showed that a similarly high number of charges are transferred for each channel during gating. Since these tetrameric associations of a single protein domain are strongly homologous to the Na^+ channel's structure, the original estimates of six charges for Na^+ channels might also be an underestimation. We therefore sought to revisit the limiting slope measurement in Na^+ channels.

Measurements of open probability (P_o) reported to date have all been made by examining the channel's response to a depolarizing pulse from the holding potential. Both the pulse protocol and the presence of noise and leak currents limit such measurements to a minimum P_o greater than about 10^{-3}, a range where modeling has shown that the slope is still changing. A greater range of measurement is therefore needed to establish a true limiting slope.

We have applied modern techniques to extend the range of P_o measurement below $\sim 10^{-7}$. The use of a skeletal muscle Na^+ channel clone deficient in fast inactivation permitted measurement of steady currents in the hyperpolarized range of potentials, and single-channel recording permitted detection of very brief open events even when very rare. Mean-Variance analysis (Patlak, 1993) was used, in part, to process hundreds of megabytes of data in order to facilitate analysis but maintain demonstrable quality. Our results show a limiting slope for Na^+ channels that is twice as steep as previously suspected, with a minimum transfer of 12 charges needed to open these Na^+ channels. These results have major implications for our understanding of Na^+ channel gating, for the estimates of the number of gates actively involved, and for the interpretation of mutagenesis experiments.

METHODS

Experiments were performed using rat skeletal muscle Na^+ channels expressed in *Xenopus* oocytes. The channel DNA and plasmid vector pRC/CMV used as starting material were a generous gift of Dr. Roland Kallen, University of Pennsylvania. We created the fast-inactivation deficient clone, IFM1303QQQ, in this channel gene after the work of West et al. (1992). Site-directed mutagenesis was performed using the pAlter kit from Promega Corp. (Madison, WI). The mutagenic oligomer was obtained from National Biosciences (Plymouth, MN) and had the sequence AGA AGT TTG GAG GGA AAG ACC AGC AGC AGA CAG AGG AAC AGA AGA AAT. The mutation and all subsequent splice sites were verified by sequencing, and three clones were generated in parallel. Since all clones behaved identically in functional assays, we assume that they contained no spurious mutations in functionally important parts of the molecule. mRNA was transcribed in vitro using standard techniques.

50–100 ng mRNA of either wild-type or noninactivating channel clones were injected into *Xenopus* oocytes previously defolliculated by treatment with 2 mg/ml collagenase-I for 1–2 h. Injected oocytes were incubated in ND96 solution containing 96 mM NaCl; 2 mM KCl; 1.8 mM $CaCl_2$; 1 mM $MgCl_2$; 5 mM HEPES; pH 7.5 supplemented with 0.54 mg/ml NaPyruvate, 100 μ/ml penicillin and 100 μg/ml streptomycin. After mechanical removal of the vitelline membrane, oocytes were placed in a depolarizing bathing solution containing 57.4 mM KAspartate; 57.4 mM CsAspartate; 3 mM $MgCl_2$; 0.18 mM $CaCl_2$; 10 mM HEPES; pH 7.4. Glass electrodes were pulled from Corning 7052 glass and filled with 140 mM NaCl; 5.3 mM KCl; 0.18 mM $CaCl_2$; 0.18 mM $MgCl_2$; 10 mM HEPES; pH 7.4. Electrode resistance was typically 2–4 MΩ.

Membrane patches were voltage-clamped using an Axopatch 200A from Axon Instruments (Foster City, CA). All experiments were performed at room temperature (21–22°C) on cell-attached patches. Steady state data was stored on a Sony DAT recorder and subsequently filtered at 7 kHz and digitized at 24 kHz. Software written by Dr. Patlak was used to perform mean-variance and half-crossing analysis of the data. Responses to short pulses were digitized and analyzed using the "Pulse" software package from HEKA Elektronik (Lambrecht, Germany).

For each patch we sought to obtain the following data: Number of channels, P_o vs potential, single-channel amplitude vs potential, and extent of slow inactivation. Current responses to brief pulses were given at the beginning and end of the protocol in order to estimate the number of channels in each patch and verify stability of the recording. Similar pulses were sometimes given in the middle of steady depolarizations to determine the extent of slow inactivation at each potential. 2–5 min of steady currents were recorded at increments of either 5 or 10 mV over a potential range from −90 to −50 mV. Recovery intervals at −100 to −120 mV of at least 1 min duration were interposed between these steady recordings in order to eliminate any residual effects of slow inactivation. Recordings at more depolarized potentials were made over shorter intervals (typically 10s of seconds) after the depolarization in order to capture the bursting activity of single

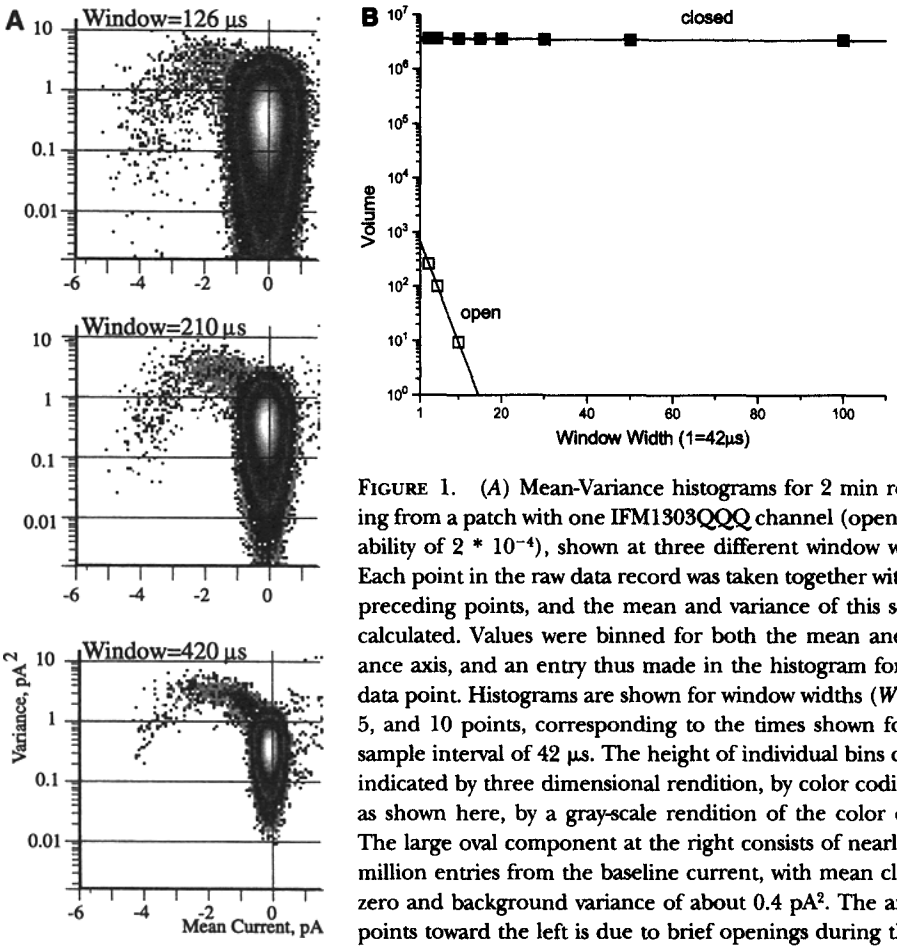

FIGURE 1. (*A*) Mean-Variance histograms for 2 min recording from a patch with one IFM1303QQQ channel (open probability of $2 * 10^{-4}$), shown at three different window widths. Each point in the raw data record was taken together with W-1 preceding points, and the mean and variance of this set was calculated. Values were binned for both the mean and variance axis, and an entry thus made in the histogram for each data point. Histograms are shown for window widths (*W*) of 3, 5, and 10 points, corresponding to the times shown for our sample interval of 42 μs. The height of individual bins can be indicated by three dimensional rendition, by color coding, or as shown here, by a gray-scale rendition of the color codes. The large oval component at the right consists of nearly four million entries from the baseline current, with mean close to zero and background variance of about 0.4 pA^2. The arch of points toward the left is due to brief openings during this recording. In those instances where the channel was open longer than the window width, one or more binned entries were made with mean values centered on the single channel current (here about −4 pA), and variance equivalent to that of the background noise. Points with high variance and intermediate mean (the arch) were due to window positions that included a transition between open and closed. (*B*) Fits to the open and closed component mean-variance volumes are plotted on semi-log axes as a function of window widths for the patch in *A*. The volumes for the closed state are nearly constant whereas they decreased strongly with window width for the open state. The time constant of this decrease is the same as the open dwell time constant, in this case 91 μs. The *y*-axis intercept (equivalent to window = one sample point) gives the predicted volume of each component in an ideal all-points histogram. Open probability for all channels (NP_o) was calculated as the ratio of the extrapolated open volume to the sum of both the open and closed volume. Final P_o estimates were obtained by dividing by *N*, the number of channels active in the patch, which was determined during strongly depolarizing pulses. In this case *N* was one, so no division was necessary.

channels before they entered their slow-inactivated state. Channel number was assumed to be one for these bursts, since simultaneous activity of a second channel would have had a high probability of showing overlapping currents. Single-channel amplitude was determined with mean-variance analysis (see below).

Our steady recordings could be analyzed in any of several different ways. Rough estimates of activity could be made by eye, for example simply by counting individual events, and thus estimating their open times and frequency. Once single-channel amplitudes were established, records with reasonable signal-to-noise, steady baselines, and no other channel activity could be analyzed using standard half-amplitude threshold crossing techniques. Finally, steady currents were usually amenable to automated production of mean-variance histograms, which permitted analysis of channel amplitude, open time, and open probability directly from the same transform.

Mean-Variance analysis was performed as in Patlak (1993). Briefly, histograms were constructed from the mean and variance of each sample point, taken together with the W-1 sequential samples immediately after (e.g., for $W = 5$ points, the mean-variance "Window" width was five points. At 24 kHz sample rate, this window spanned 0.21 ms). Mean-Variance data pairs were binned in mean direction, and log-binned in the variance direction to form a Mean-Variance histogram, as illustrated in Fig. 1 *A* for window widths ranging from 3 to 10 points (0.126–0.42 ms). The number of entries in each bin were encoded by the color, rendered here in gray-scale. The large component of each histogram that is centered at 0 pA is the baseline current. Its variance is due to background noise. Channel openings cause points to arch to the left. Those instances where the channel was open longer than the window width caused entries with variance as low as the baseline, and with mean amplitude of the single-channel current, in this case about 4 pA.

Open probability was determined as follows: the volume (total number of entries in all the bins that comprise each component) of the zero-current component was determined by fitting to Gaussian and χ^2 functions as described in Patlak (1993). For the open component at low P_o, the volume was estimated under the assumption that the variance distribution of the open state was not significantly different from that of closed channels. Bins below the median variance of the open component were summed and the result was doubled to obtain the final volume estimate. Open and closed state mean-variance volumes were plotted on semi-log axes as a function of window width as shown in Fig. 1 *B*. The volumes for the closed state were nearly constant, indicating that closed dwell times were usually much longer than the longest window width used. The volume for the open times decreased strongly with window width. The time constant of this decrease is the same as the dwell time constant, in this case 91 μs. The *y*-axis intercept (equivalent to window = 1 sample point) gave the predicted volume of each component in an all-points histogram. Open probability for all channels (NP_o) was calculated as the ratio of the extrapolated ($W = 1$) open volume to the sum of both the open and closed volume. Final P_o estimates were obtained by dividing by N, the number of channels active in the patch, which was determined during strongly depolarizing pulses. Since the same value for N was used for all recordings in a patch, errors in its estimation would not influence the slope of the P_o curve. In the case of this patch, N was one, and P_o was calculated to be $1.3 * 10^{-4}$.

Fast (in wild-type channels) and slow inactivation were measured using standard pulse protocols. In brief—fast inactivation: pulses to 0 mV were applied at 1 Hz from a holding potential of −100 to −120. 20-ms conditioning pulses were given to various potentials, and the resulting peak current was plotted as the fraction of current without conditioning. Slow inactivation: the membrane potential was held at various potentials for 1 min, then pulses to 0 mV were given after a 20-ms recovery prepulse to −120 mV. The recovery prepulse removed any residual fast inactivation, if present. Data were plotted as the ratio of peak current to that seen when the holding potential was −120 mV.

RESULTS

Our initial attempts to measure limiting slope were made on wild-type skeletal muscle Na^+ channels, either in their native tissue, or expressed in mammalian cells or oocytes. Brief single-channel openings can be resolved in all these preparations at potentials as negative as −100 mV. The results illustrated here for wild-type channels expressed in *Xenopus* oocytes are typical. Fig. 2 *A* shows raw steady currents at

three potentials recorded from an oocyte patch with ~30 wild-type channels. Each trace shows 50 s of recording by compressing the actual sample points into 1,000 vertical bars, each of which represent the maximum and minimum currents recorded during 50 ms (i.e., peak to peak currents). The openings of Na^+ channels are seen as brief downward deflections of current. When a vertical bar containing one of these openings is expanded to show the full 50 ms (see inset above the first trace), the actual opening can be seen more clearly. Finally, if this trace is further expanded to show just 2 ms of data, the single opening can be fully resolved.

Qualitatively, one can see a clear increase in the frequency of such currents from −90 to −85 mV. Just counting events gives a nearly 10-fold increment over this range of potential. A further increment is seen between −85 and −80 mV, but the difference is not as large. When these data were quantified with either half amplitude threshold analysis or mean-variance histograms (shown for these data in Fig. 2 *B*), channel open probabilities and open times could be determined.

Fig. 3 *A* shows open probability and open time for these wild-type channels. Consistent with the qualitative estimates described above, the P_o curve shows a steep increase in currents between −90 and −85 mV, but then becomes nearly level at more positive potentials. Open times were ~0.1 ms over the whole voltage range, with a gradual increase (roughly e-fold/25 mV) in the range from −90 to −70 mV. Although the results at the most negative potentials are suggestive of a steep limiting slope, the inactivation process appears to mask the activation behavior over most of the measurable range of potentials.

We measured both fast (H_∞) and slow (S_∞) inactivation voltage dependence in this preparation. Fig. 3 *B* shows the position of these curves. Both forms of inactivation had effects at potentials more depolarized than −80 mV. These two forms of inactivation, plus any other additional components that were not quantified in our measurements were responsible for reducing steady P_o for these Na^+ channels to $\sim 10^{-5}$.

Because two or more additive inactivation processes were active, and because each is difficult to quantify separately, correction for inactivation would be of dubious value in this preparation. Furthermore, such measurements cannot be made during the interval before inactivation is complete (e.g., a pulse response) because average closed dwell times for channels in the most negative range of potentials reach 10s of seconds. Therefore, it was impossible to make such measurements in normally inactivating channels. Instead, we sought to express Na^+ channels that were mutated in a way that removed fast inactivation.

Fig. 4 *A* shows 2-s records of currents through skeletal muscle Na^+ channels with the IFM1303QQQ mutation of West et al. (1992). As the potential became more depolarized, currents switched as a function of membrane potential from dominant closed times with brief openings to prolonged bursts where the open state is predominant. These channels lacked nearly all fast inactivation process, although they retained slow inactivation, which terminated the bursting responses at the more depolarized potentials.

The activation kinetics of this channel clone were essentially normal. Fig. 4 *B* shows average currents from wild-type and mutant channels, along with a peak current-voltage curve. Although the mutant channels did not express as well as wild type, and thus did not attain equivalent current densities, the sensitivity of the channels to volt-

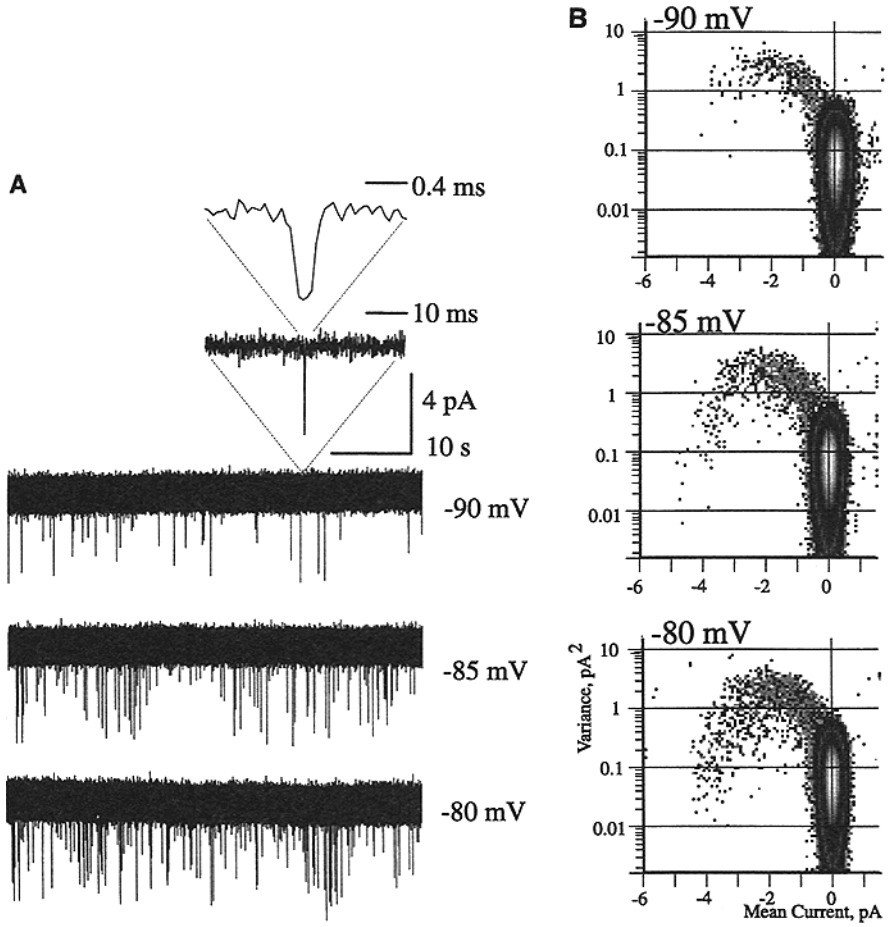

FIGURE 2. (*A*) 50 s steady state recordings of wild-type sodium channel activity at three potentials in a patch with at least 16 channels. Each trace consists of 1,000 vertical lines that span the minimum to maximum (peak-to-peak) currents recorded during 50 ms of activity. The 1,200 sample points taken during one of these lines are expanded above the trace at −90 mV, centered on an opening. The opening itself is clearly seen when the trace is further expanded to show 2 ms of activity. In the case of this opening, the event duration was ~0.2 ms. (*B*) Mean-variance histograms of the recordings shown in *A*. The construction and scaling of these histograms is identical to that described in Fig. 1.

age, as well as their activation time course were nearly identical to those of the wild type.

We have measured the steady state voltage dependence of P_o in the IFM1303-QQQ mutant channel. The raw currents at the most negative potentials were qualitatively identical to those shown above in Fig. 2 *A*, but the currents from this channel continued to increase to high levels of open probability as the potential became more depolarized. P_o values are shown in Fig. 5 *A* as a function of membrane potential. The closed squares in the main graph show open probability in one patch

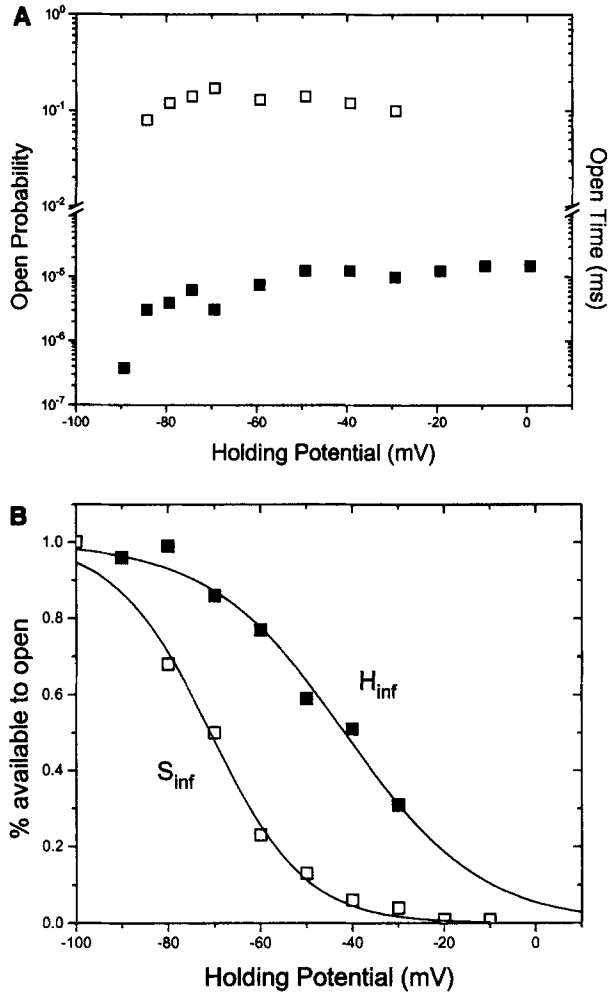

FIGURE 3. (*A*) Open probability in wild-type skeletal muscle Na^+ channels as measured with the mean-variance technique (*filled squares*; see Fig. 1, *A* and *B*, for methods) and open-dwell time (*open squares*) measured with half-amplitude threshold crossing, as a function of steady state holding potential. The scale for the open time axis is the same as that for the open probabilities. (*B*) The voltage sensitivity of fast and slow inactivation. Fast inactivation (h_∞) was defined by the relative peak current during a test pulse to 0 mV after a conditioning pulse of 20 ms duration to the potential shown in the graph. Slow inactivation (S_∞) was measured as the relative peak current remaining when the membrane potential was held constant at the potential shown. The test potential to 0 mV followed a 30-ms prepulse at −120 mV to permit recovery from fast inactivation. The solid lines represent Boltzman fits to the data.

in which we covered the full range of potentials in 10-mV steps. The open squares show the results from another patch in which the more negative potentials were measured with 5-mV increments (these latter data have been shifted on the voltage axis, see figure legend).

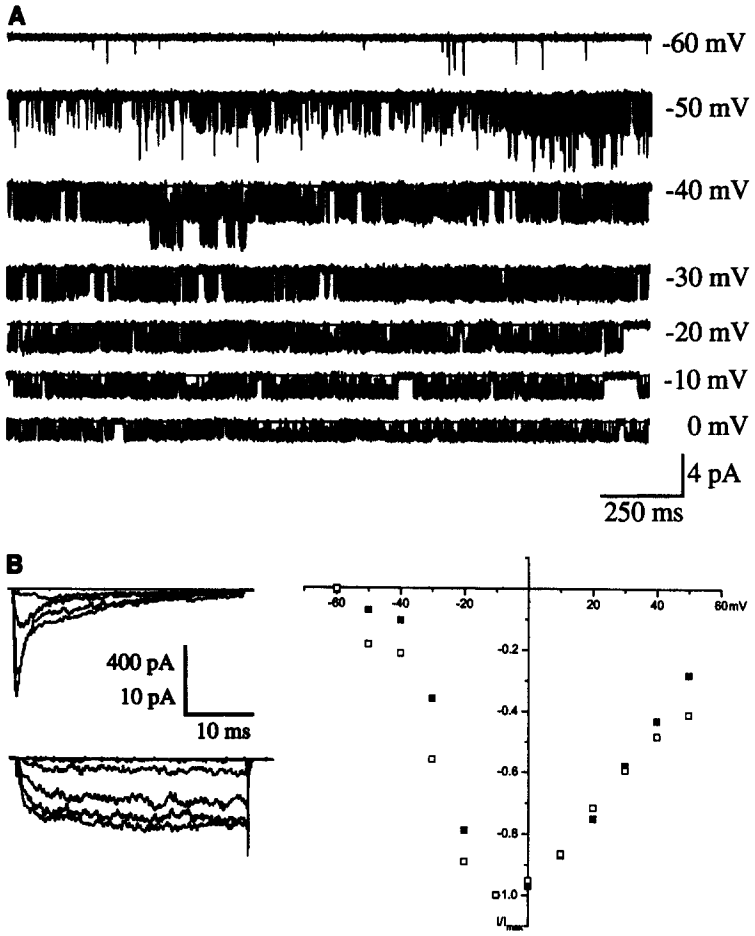

FIGURE 4. (*A*) Two second recordings of the activity of the mutant IFM1303QQQ Na^+ channels expressed in *Xenopus* oocytes at different holding potentials. (*B*) (*Left*) Current elicited by individual 30-ms pulses to potentials from −60 to −10 mV (10-mV increments) from a holding potential of −100 mV for wild-type (*top*) and IFM1303QQQ (bottom, average of five pulses for each trace) sodium channels. (*Right*) Peak current-voltage relationship derived from the traces like those shown. Currents were normalized to 1 at −10 mV for wild-type (*solid squares*) and IFM1303QQQ (*open squares*).

Between −80 and −70 mV the open probability increased ~100-fold. Furthermore, over the next 10 mV (between −70 and −60) P_o increased another 100-fold. The limiting slope was thus maintained over a range of 10,000-fold increase in P_o. The straight line was fitted by eye to this limiting range between −80 and −60 mV. It has a slope of e-fold increase per 2.2 mV (equivalent gating charge of about 11.4 e^-). We have seen slopes as steep as this in nearly every patch we have analyzed, with an average slope of e-fold per 1.97 mV ± 0.22 mV SD ($N = 7$) with an average effective charge of 12.7 e^-, as shown in the inset to Fig. 5 *A*. Note that the exact position of the P_o curve on the voltage axis was variable from cell to cell. This effective

voltage but not the slope was also modified by agents affecting protein kinase C (Hirschberg et al., 1995). Nevertheless, the slope appeared to be consistently as expected for ~12 effective gating charges.

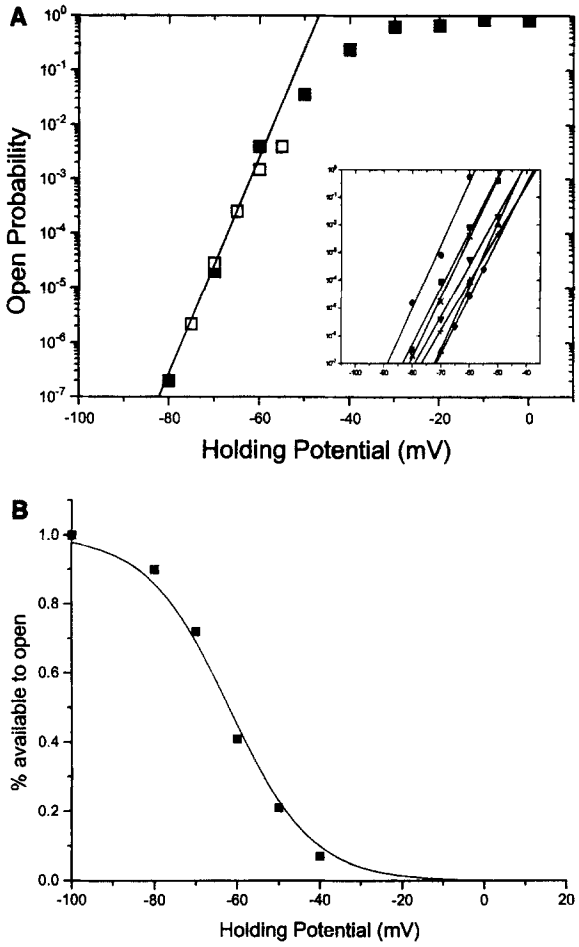

FIGURE 5. (*A*) Voltage-dependence of the steady state open probability of IFM1303QQQ as derived from mean-variance analyses. The solid line is fit to the most hyperpolarized data points with a steepness factor of e-fold per 2.2 mV. The filled squares are derived from one patch using measurements at 10-mV intervals to span the full range of probabilities. The open squares are from another patch, sampling the steep region of the curve at 5-mV intervals. (Due to the variability in activation potential from one cell to the next, the open squares have all been shifted by −10 mV so that they match the voltage range observed in the first patch.) The inset shows raw data from seven different patches recorded in the same conditions. In each case, the solid lines show the best fit to the lowest 20 mV of the activation curve. Despite the variability in effective activation potential, the slope was very consistent from cell to cell. (*B*) Slow inactivation in IFM1303QQQ channels (S_∞) as a function of holding potential. Relative inactivation was measured as in Fig. 3, with currents normalized to the peak response when holding potential was −120 mV. Open probabilities were not corrected for this slow inactivation. The effect of any such correction would be to add steepness to the P_o curve.

These data were not corrected for the effects of slow inactivation, which was still present in this preparation. We measured slow inactivation as described above for the wild-type channels by determining peak current responses to strongly depolarizing pulses (e.g., to 0 mV) after several minutes at various holding potentials. Fig. 5 *B* shows an example of such a slow inactivation curve. Slow inactivation caused diminution of the steady currents ranging from ~0.9 at −80 to ~0.4 at −60. Note that correction for such slow inactivation would further steepen the limiting slope. The net effect of such correction would be to add another effective charge to the 12 estimated above.

The observation was not the result of missed open events. Fig. 6, *A* and *B*, show the distribution of open and closed times from a patch with four channels at −60 mV using half amplitude threshold crossing analysis. 150 s of data were filtered at 5 kHz and sampled at 48 kHz for this record. The open time histogram contained 661 events that crossed half amplitude, with a best fitting single exponential time constant of 149 μs (note that the distribution is somewhat distorted from the ideal exponential shape, due to the large number of very brief events), giving a P_o for this patch of $1.7 * 10^{-4}$. As with most of our patches where both half amplitude and mean-variance methods could be accurately performed, open times and probabilities agreed closely. For the data shown here, mean-variance analysis gave values of 162 μs and $1.4 * 10^{-4}$ for open time constant and P_o, respectively. These measurements show that at −60 mV the open time constant was about six times the "dead time" for half-amplitude crossing at our standard filter setting of 7 kHz.

Fig. 6 *C* shows measurements of open time constants as a function of potential. Note that the voltage dependence of the open state (e-fold per 25 mV, or 1.0 e^-) was much lower than the steepness factor for the overall P_o. Therefore we would not expect that our sharply declining P_o's at hyperpolarized potentials were artifactually produced by progressive failure to detect openings in this range of potentials. For example, at −85 mV, our data indicate that the mean open time should still be ~50 μs, or twice the expected "dead time" for the recording. As had been previously shown by Hoshi et al. (1994) for single K^+ channel records, this steepness was due to changes in the closed times, as expected for models in which most of the gating charge is exchanged during transitions between multiple closed states.

DISCUSSION

We report here that the voltage sensitivity of activation in Na^+ channels at the hyperpolarized extreme is consistent with a minimum of 12 charges crossing the membrane's field. This result is significant for a number of reasons. For the past 40 years, it has been assumed that half that number of charges were involved in Na^+ channel activation. Most models (for example, see recent reviews by Patlak, 1991; Sigworth, 1994; Keynes, 1994) have been built and carefully tuned with the lower number of charges, and our result will force a reevaluation of the ability of these models to describe the data quantitatively. Finally, any model of the channel's structure/function relationship is significantly constrained by the necessity for moving such a large amount of charge through the membrane. These issues are discussed in more depth below.

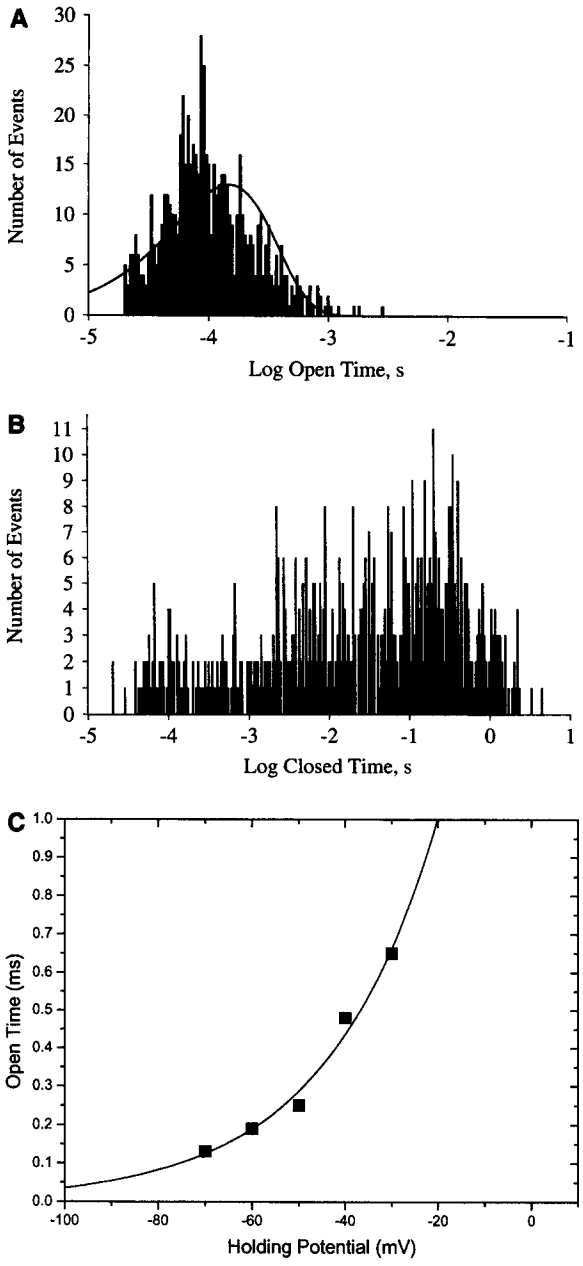

FIGURE 6. (*A*) Open time histogram for a 2.5-min steady state recording at −60 mV. Data were filtered at 5 kHz and sampled at 48 kHz, then analyzed using the half-amplitude threshold crossing method and fit to a single exponential distribution as shown by the solid line (661 total open events; open time constant of 0.149 ms). (*B*) Closed time histogram for the same recording as in *A*. (*C*) Open times as a function of voltage. Data were fit to a single exponential with a steepness factor of e-fold increase per 25 mV.

Our observations are different from those from previous reports because we have strongly enhanced the resolution of measurement with a combination of techniques. Previous measurements were constrained to look at P_o values $>\sim 10^{-3}$ because they examined macroscopic currents during brief pulses. Measurements of very small macroscopic currents are difficult because they require all other sources of current be either eliminated or subtracted. As currents become smaller, the relative errors in such procedures become larger. Furthermore, during pulses in the extreme hyperpolarized range, the time necessary to activate the channels fully may drastically exceed the length of the pulse. Such constraints severely limit the ability to resolve P_o values at their true limit of voltage sensitivity.

By using single-channel recording, we were able to distinguish Na^+ channel currents by their unitary amplitude, regardless of how often individual events occurred. In a quiet patch, for example, a single 0.1 ms opening could easily be detected at our 7-10 kHz filter frequency (especially when its amplitude is >4 pA as at −90 mV), and could still be quantified even if it occurred only once per minute. This would correspond to a P_o of $\sim 2 * 10^{-6}$. For a patch with more than one channel, the activity measured would be represented by NP_o, where N is the number of channels present. Patches in oocytes often had >10 channels, yielding minimum P_o resolution of $<10^{-7}$ when the measured probability is divided by the number of channels present. Therefore, single-channel recording has the ability to extend P_o measurements by four orders of magnitude. This is precisely the range of values where the slope becomes truly limiting.

These observations can be made with standard analysis techniques, although they require processing large amounts of data with demonstrable reliability. Each minute of recording uses ~3 megabytes of storage. These files must be checked for baseline stability and extraneous channel activity, then processed to determine Na^+ channel amplitude, duration, and frequency. This task was made easier using mean-variance analysis, which condensed minutes of data into a small set of two-dimensional mean-variance histograms. Such histograms display the quality of the data, and permit subsequent analysis of both open times and P_o for components with defined amplitude. Use of this technique greatly facilitated obtaining data of the highest quantity and quality.

Finally, we used the tools of molecular biology to generate and express a channel variant permanently lacking fast inactivation. Enzymatic approaches to removing fast inactivation are highly nonspecific, producing a potentially heterogeneous population of channels that may have other alterations as well. The IFM1303QQQ mutation, in contrast, is identical for each expressed channel, and appears to be relatively specific in its removal of fast inactivation. The combined use of single-channel recording, mean-variance analysis, and mutagenesis therefore permitted an extension of our resolution into a completely new range.

Our observation of 12 effective charges does not appear to be an artifact of the methods used to measure the currents. Channel open times are brief in this hyperpolarized range, but still long enough that most events can be resolved and quantified. Furthermore, since the open times are much less strongly dependent on voltage, the rapid and consistent diminution of activity could not be due to the openings becoming vanishingly short. Rather, they simply became further and further apart.

If the limiting slope were less steep than we measured, then we should have seen orders of magnitude greater activity at the most negative potentials. For example, a "limiting" slope of e-fold/4 mV (six charges) fits our data between −60 and −40 mV. Extending this curve to −80 mV would give a P_o of $8 * 10^{-5}$, or 400-fold higher than we actually saw. Since this extra activity was absent, we must conclude that the slope could not have been as low as six effective charges.

Although our measurements for these Na^+ channels extend the measurable range and show a higher limiting slope, they do not contradict previous estimates. As indicated above, our data also show a slope of six charges in the range of 0.1 to 0.001, where most previous estimates of limiting slope were derived. For skeletal muscle Na^+ channels, however, this range is not sufficiently negative to reach the true limit.

Even though Hodgkin and Huxley originally measured a limiting slope of about six charges, their model of Na^+ channel kinetics used a number nearly as high as we measured. The steepness factors for α_m and β_m would give each hypothetical "m" particle an effective charge of 3.4–3.9 in the hyperpolarized potential range. Three such particles would thus have a total gating charge of 10–12 charges. Note however that the limiting slope of the Hodgkin and Huxley model is only reached at very negative potentials; at the lower limit of our resolution, the Hodgkin-Huxley equations have not yet reached their limit, only predicting 9.8 charges between −80 and −70 mV. The deviation from the true limiting slope at these potentials is due primarily to the nonexponential terms in their equation for α_m.

The use of 12 or more charges places significant constraint on either kinetic or structure/function models of the Na^+ channel. Each S4 segment (the putative voltage sensors and source of the gating charge) has five to seven charges over its entire length. For a membrane-spanning array of seven charges located in a linear field, complete movement of the entire segment out of the field would transfer about four charges. It is therefore impossible to transfer 12 or more charges with fewer than three S4 segments. The participation of all four S4 segments, each with about three effective charges, appears more reasonable, and is also more consistent with fluctuation estimates of the "quantal" gating charge of 2.4 e^-/gate (Conti and Stühmer, 1989).

The effect of S4 charges mutation on voltage sensitivity has generally been made at relatively depolarized pulse potentials, where the steepness of the P_o curve is much less than the limit we observed. The significant alterations that were seen (e.g., Stühmer et al., 1989) could not have been due to alteration of one charge in 12 (an 8% reduction). Rather, the gating in this depolarized range must be due to the preferential activity of a subset of gates, possibly explaining why mutations to the S4's in different domains show variable effects on this measured slope. Reexamination of such mutations with higher resolution of P_o will be critical in sorting out such specialized roles of the channel's domains.

We cannot, at present, state that our result for skeletal muscle Na^+ channels is directly applicable to all Na^+ channel subtypes. Since the gates that participate in activation need not be identical to one another in effective charge or midpoint of activity, preparations could differ in both the shape and slope of the P_o curve. For example, if a channel subtype had one of its gates "locked" in an open position, then

that gate would not transfer any charge during depolarization. The channel would have a lower limiting slope. Similarly, channels with gates that moved over drastically different potential ranges might show P_o curves with more curvature, gradually increasing in slope over a broad range of potential. Until we have examined other channel subtypes, we can only say that all the gates of the skeletal muscle Na^+ channel subtype appear active and well "tuned" to one another. Further structure/function studies will be needed to clarify our image of this complex channel.

The authors wish to thank Dr.'s Richard Horn and Mark Nelson for helpful comments on the manuscript, and Dr. Roland Kallen for his gift of Na^+ channel DNA.

This work was supported by an NIH grant to Dr. Patlak. Dr. Hirschberg was supported by a fellowship from the Vermont Affiliate of the American Heart Association.

Original version received 21 June 1995 and accepted version received 15 August 1995.

REFERENCES

Aggarwal, S. K., and R. MacKinnon. 1995. A comparison of the gating charge per channel of the *Shaker* and DRK1 K^+ channels. *Biophysical Journal.* 68:138*a*. (Abstr.)

Almers, W. 1978. Gating currents and charge movements in excitable membranes. *Review of Physiology and Biochemical Pharmacology.* 82:97–190.

Conti, F., and W. Stühmer. 1989. Quantal charge redistributions accompanying the structural transitions of sodium channels. *European Biophysical Journal.* 17:53–59.

Hirschberg, B., M. Lieberman, A. Rovner, and J. Patlak. 1995. Modulation of wildtype and noninactivating skeletal muscle sodium channels expressed in xenopus oocytes by Protein Kinase C. *Biophysical Journal.* 68:48*a*. (Abstr.)

Hodgkin, A. L., and A. F. Huxley. 1952*a*. Currents carried by sodium and potassium ions through the membrane of the giant axon of *Loligo*. *Journal of Physiology.* 116:449–472.

Hodgkin, A. L., and A. F. Huxley. 1952*b*. A quantitative description of membrane current and its application to conduction and excitation in nerve. *Journal of Physiology.* 117:500–544.

Hoshi, T., W. N. Zagotta, and R. W. Aldrich. 1994. *Shaker* posassium channel gating I: transitions near the open state. *Journal of General Physiology.* 103:249–278.

Noda, M., T. Tanabe, T. Takai, T. Kayano, T. Ikeda, H. Takahashi, H. Nakayama, Y. Kanaoka, N. Minamino, K. Kangawa, H. Matsuo, M. A. Raftery, T. Hirose, S. Inayama, H. Hayashida, T. Mayata, and S. Numa. 1984. Primary structure of Electrophorus electricus sodium channel deduced from cDNA sequence. *Nature.* 312:121–127.

Oxford, G. S. 1981. Some kinetic and steady-state properties of sodium channels after removal of inactivation. *Journal of General Physiology.* 77:1–22.

Patlak, J. 1991. Molecular kinetics of voltage-dependent Na^+ channels. *Physiological Reviews.* 71:1047–1080.

Patlak, J. 1993. Measuring kinetics of complex single ion channel data using mean-variance histograms. *Biophysical Journal.* 65:29–42.

Schoppa, N. E., K. McCormack, M. A. Tanouye, and F. J. Sigworth. 1992. The size of gating charge in wild-type and mutant *Shaker* potassium channels. *Science.* 255:1712–1715.

Sigworth, F. J. 1994. Voltage gating of ion channels. *Quarterly Reviews of Biophysics.* 27:1–40.

Stimers, J. R., F. Bezanilla, and R. E. Taylor. 1985. Sodium channel activation in the squid giant axon. Steady state properties. *Journal of General Physiology.* 85:65–82.

Stühmer, W., F. Conti, H. Suzuki, X. Wang, M. Noda, N. Yahagi, H. Kuo, and S. Numa. 1989. Struc-

tural parts involved in activation and inactivation of the sodium channel. *Nature.* 339:597–603.

West, J. W., D. E. Patton, T. Scheuer, Y. Wang, A. L. Goldin, and W. A. Catterall. 1992. A cluster of hydrophobic amino acid residues required for fast Na^+ channel inactivation. *Proceedings of the National Academy of Sciences, USA.* 89:10910–10914.

Zagotta, W. N., T. Hoshi, J. Dittman, and R. W. Aldrich. 1994. *Shaker* potassium channel gating II: Transitions in the activation pathway. *The Journal of General Physiology.* 103:279–319.